Eur. Phys. J. B **16**, 345–353 (2000)

THE EUROPEAN PHYSICAL JOURNAL B

EDP Sciences

Diffusion and electromigration on disordered surfaces

U. Börner[a] and J. Krug[b]

Fachbereich Physik, Universität GH Essen, 45117 Essen, Germany

Received 7 February 2000

Abstract. We study a one-dimensional disordered solid-on-solid model in which neighboring columns are shifted by quenched random phases. The static height-difference correlation function displays a minimum at a nonzero temperature. The model is equipped with volume-conserving surface diffusion dynamics, including a possible bias due to an electromigration force. In the case of Arrhenius jump rates a continuum equation for the evolution of macroscopic profiles is derived and confirmed by direct simulation. Dynamic surface fluctuations are investigated using simulations and phenomenological Langevin equations. In these equations the quenched disorder appears in the form of time-independent random forces. The disorder does not qualitatively change the roughening dynamics of near-equilibrium surfaces, but in the case of biased surface diffusion with Metropolis rates it induces a new roughening mechanism, which leads to an increase of the surface width as $W \sim t^{1/4}$.

PACS. 68.35.Fx Diffusion; interface formation – 05.70.Ln Nonequilibrium and irreversible thermodynamics – 61.43.Dq Amorphous semiconductors, metals, and alloys

1 Introduction and outline

At temperatures not too close to the melting point, solid surfaces relax towards equilibrium primarily through surface self-diffusion [1]. As a consequence, surface diffusion plays a central role in the morphological evolution of surfaces also far from equilibrium, because it provides the dominant smoothening mechanism counteracting the destabilizing nonequilibrium fluxes. The activation energy for surface diffusion therefore governs the temperature dependence of the characteristic length and time scales of diverse morphological phenomena such as ripples induced by ion sputtering [2] and electromigration-induced shape transitions of voids in thin films [3].

Microscopic approaches to surface diffusion typically consider the migration of adsorbed atoms (adatoms) on a perfect crystalline surface composed of atomically flat terraces and monoatomic steps [4]. Much less appears to be known about diffusion on amorphous surfaces [5], despite the fact that the role of surface diffusion in the large-scale evolution of amorphous films is well documented [2,6,7]. Conceptually, self-diffusion on amorphous surfaces is an intriguing problem in that it adds to the rich phenomenology of diffusion in a disordered environment [8] the additional complication that the environment is built up of the diffusing species, and hence evolves in response to the diffusion process [9].

In this paper we explore some aspects of diffusion on amorphous surfaces in the framework of the one-dimensional phase-disordered solid-on-solid (DSOS) model [10–12]. The choice of this – clearly oversimplified – model is motivated by our interest in establishing a reasonably stringent connection between microscopic dynamics and macroscopic evolution, which is a very hard problem for more realistic models. The DSOS model includes structural disorder only in the direction perpendicular to the surface, while maintaining an ordered lattice along the surface. Its equilibrium properties are governed by the Hamiltonian

$$\mathcal{H}_{\mathrm{DSOS}} = K \sum_i |h_i + \phi_i - h_{i-1} - \phi_{i-1}|, \qquad (1)$$

where $K > 0$ is the bond energy divided by $k_{\mathrm{B}}T$, the h_i are integer height variables defined above the points i of the one-dimensional substrate lattice and the *phases* ϕ_i are independent random variables uniformly distributed in $[-1/2, 1/2]$. The ϕ_i describe the random offsets between neighboring columns of the two-dimensional solid (see Fig. 1). They introduce quenched disorder into the model: thermodynamic quantities are computed for a fixed configuration of phases, and subsequently a disorder average is performed.

The near-equilibrium behavior of the two-dimensional DSOS model and its continuum analog, the phase-disordered sine-Gordon model, has been extensively studied in the past [11,13–15]. It displays a glass transition connecting a conventionally rough high-temperature phase to a "superrough" low temperature phase, which

[a] *Present address:* MPI für Physik komplexer Systeme, Nöthnitzer Str. 38, 01187 Dresden, Germany

[b] e-mail: jkrug@theo-phys.uni-essen.de

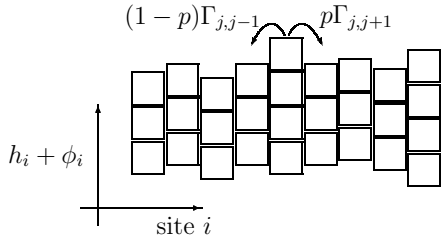

Fig. 1. Illustration of the one-dimensional phase-disordered SOS model with surface diffusion dynamics.

replaces the roughening transition of the pure SOS model. In the one-dimensional case no such transition occurs. However, as we will show in Section 2, the surface roughness displays a minimum at a nonzero temperature, which marks in a similar way the transition from the entropically dominated high-temperature regime to disorder-dominated low temperature behavior.

In Section 3 the DSOS model is equipped with a volume-conserving dynamics which allows the topmost particle in each column to hop to the neighboring columns with rates satisfying detailed balance with respect to $\mathcal{H}_{\rm DSOS}$. The large scale dynamics of the surface is then governed by a continuum equation of the form [1]

$$\frac{\partial h}{\partial t} = -\frac{\partial}{\partial x}\sigma\frac{\partial}{\partial x}\hat{\gamma}\frac{\partial^2 h}{\partial x^2}, \tag{2}$$

where $h(x,t)$ describes the surface profile and the properties of the microscopic model enter in the *surface stiffness* $\hat{\gamma}$ and the adatom mobility σ, both of which are (in general) functions of the local surface slope $\nabla h = \partial h/\partial x$. In [16] an exact derivation of (2) from the microscopic dynamics was carried out for the ordered SOS model. In Section 3 this procedure is adapted to the disordered model, and the validity of the continuum equation (2) (with appropriately disorder averaged stiffness and mobility) is demonstrated through simulations of surface profile relaxation.

In Section 4 the surface is driven out of equilibrium by imposing a bias on the surface diffusion jumps. Physically such a bias can be thought to arise from an electric bulk current, which induces electromigration of surface atoms [17,18]. Previous studies of the ordered system have shown that electromigration-induced mass transport stabilizes or destabilizes the surface depending on the relative orientation of driving force and surface slope [19,20]. Here we focus on the case of stabilization. In the absence of disorder the bias then completely suppresses the thermal surface roughness, such that the width W of a surface of length L becomes independent of L [19] (for a one-dimensional equilibrium surface $W \sim L^{1/2}$).

This behavior changes qualitatively in the presence of disorder. The disorder roughens the surface such that in the stationary state $W \sim L^{1/2}$, while the temporal roughness buildup from a flat initial condition follows the power law $W \sim t^{1/4}$, *faster* than the corresponding equilibrium behavior $W \sim t^{1/8}$ [16]. The origin of this novel effect is a quenched random contribution to the adatom mobility σ appearing in (2). Together with the external driving force it gives rise to a quenched random current. In the steady state the spatial variations of the random current must be compensated by chemical potential gradients, which implies a corresponding deformation of the surface.

Similar large scale effects of quenched random mobilities have been discussed previously in different contexts [12,21,22], but in the present model the behavior appears to be particularly simple and clearcut. The roughening dynamics can be quantitatively described by a linear continuum theory, and the steady state surface deformation can be predicted directly from the microscopic disorder configuration, at least for temperatures which are not too low. The paper closes with some conclusions in Section 5.

2 Static properties

The identification of the quantities which appear in the continuum equation (2) requires some preliminary work, namely the calculation of equilibrium averages (such as the stiffness $\hat{\gamma}$) at fixed surface inclination. This is done most conveniently in a grand canonical scheme, where a term involving a site-dependent chemical potential μ_i is added to the Hamiltonian (1) [16]. The total energy then reads

$$\begin{aligned}\mathcal{H} &= \mathcal{H}_{\rm DSOS} - \sum_i \mu_i(h_i + \phi_i) \\ &= K\sum_i |u_i + \Delta_i| - \sum_i m_i(u_i + \Delta_i),\end{aligned} \tag{3}$$

where $u_i = h_i - h_{i-1}$ is (the integer part of) the local slope, $\Delta_i = \phi_i - \phi_{i-1}$ is the random phase shift between the neighboring columns, and the slope chemical potential m_i is related to the standard chemical potential through $\mu_i = -(m_i - m_{i-1})$. As defined, the Δ_i display nearest neighbor correlations. However since the model is invariant under arbitrary local integer shifts of the Δ_i, a transformation can be found which replaces them by uncorrelated random variables uniformly distributed in $(-1/2, 1/2)$ [23].

Since (3) describes a system of noninteracting slope variables, it is straightforward to compute the partition function and to obtain moments of the local slope u_i by taking derivatives with respect to m_i. In the following we will need the thermal average of the slope $\langle u_i\rangle$ and its variance

$$\langle u_i^2\rangle - \langle u_i\rangle^2 = \frac{\partial}{\partial m_i}\langle u_i\rangle, \tag{4}$$

both of which are functions of m_i and Δ_i; explicit expressions can be found in [23].

2.1 Disorder-averaged stiffness

The surface stiffness of the ordered SOS model is obtained [16] by taking the continuum limit of the relations

$u_i = h_i - h_{i-1}$ and $\mu_i = -(m_i - m_{i-1})$ and using the chain rule, which yields

$$\mu(x) = -\frac{\partial m}{\partial x} = -\frac{\mathrm{d}m}{\mathrm{d}u}\frac{\partial u}{\partial x} = -\left(\frac{\mathrm{d}u}{\mathrm{d}m}\right)^{-1}\frac{\partial^2 h}{\partial x^2} = -\hat{\gamma}\frac{\partial^2 h}{\partial x^2}, \tag{5}$$

and identifies the stiffness with the inverse of the variance of the slope. Clearly this approach requires that for a slowly varying surface (or slope) profile also the slope chemical potential m is slowly varying. In the presence of phase disorder this is no longer true due to the additional dependence on the random shifts Δ_i. The relation between u and m therefore has to be smoothened by performing the disorder average *before* taking the continuum limit. The macroscopic stiffness of the DSOS model is then given by

$$\overline{\hat{\gamma}} = \left(\frac{\mathrm{d}\overline{\langle u\rangle}}{\mathrm{d}m}\right)^{-1}, \tag{6}$$

where the overbar implies disorder averaging.

According to (6), the stiffness is the inverse of the disorder averaged slope variance. Alternatively one might consider defining it as the disorder average of the inverse of the variance. The two quantities differ considerably at low temperatures [23]. As we will show in Section 3, simulations of profile relaxation allow us to unambiguously decide in favor of the definition (6).

The explicit evaluation yields the expressions

$$\overline{\langle u\rangle}(m) = \frac{1}{2K}\left(\frac{K\sinh m + m\sinh K}{\cosh K - \cosh m}\right) \tag{7}$$

and

$$\overline{\hat{\gamma}}^{-1}(m) = \frac{K(m\cosh K - 1) + \sinh K(\cosh K - \cosh m + m\sinh m)}{2K(\cosh K - \cosh m)^2}, \tag{8}$$

both of which hold for $|m| \le K$. Together equations (7, 8) define a parametric representation of $\overline{\hat{\gamma}}(u)$. The temperature dependence of the stiffness differs qualitatively from that of the ordered SOS model (Fig. 2). In particular, for $m = 0$ ($u = 0$) it behaves as $\overline{\hat{\gamma}} \approx 2K$ for $K \to \infty$ in contrast to the exponential divergence $\hat{\gamma}_{\mathrm{SOS}} \sim \mathrm{e}^K$ in the ordered case. In the high temperature regime, $\overline{\hat{\gamma}}$ converges to $\hat{\gamma}_{\mathrm{SOS}}$. The inclination dependence of the stiffness is qualitatively similar both in the ordered and disordered case, $\overline{\hat{\gamma}} \to u^{-2}$ for $u \to \infty$, but with a broader maximum at $u = 0$ for the disordered model in the low temperature regime.

2.2 Height difference correlation function

In the SOS model the height difference correlation function

$$C(r) := \frac{1}{L}\sum_{j=0}^{L-1}\overline{\langle (h_{j+r} - h_j)^2\rangle} \tag{9}$$

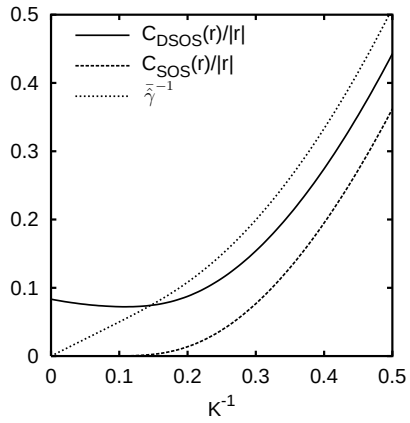

Fig. 2. Temperature dependence of the coefficient of the height-difference correlation function $C(r)/|r|$ in the DSOS model (full line) and the SOS model (dashed line) at zero mean slope ($m = 0$). The dotted line is the inverse stiffness $(\overline{\hat{\gamma}})^{-1}$ of the disordered model. In the SOS model $C(r)/|r| = \hat{\gamma}^{-1}$.

is directly connected to the stiffness, since $C(r) = |r|/\hat{\gamma}$. In the disordered system one has additional contributions which are due to the random phase shifts, and

$$C(r) = (\overline{\langle u^2\rangle} + 2\overline{\langle u\rangle\Delta} + \overline{\Delta^2})|r|. \tag{10}$$

The last term $\overline{\Delta^2} = 1/12$ reflects the roughness of the ground state of (1) [10] and is the only one that survives at zero temperature. For $u = 0$ the first term can be identified with the inverse stiffness, while the second, mixed term is given by the integral

$$\overline{\langle u\rangle\Delta} = -2\int_0^{1/2}\mathrm{d}\Delta\frac{\Delta\sinh K\Delta}{\sinh K(1-\Delta) + \sinh K\Delta}\,. \tag{11}$$

It is negative, which shows that the system tries to compensate the imposed phase shift through a corresponding inclination of the opposite sign in order to minimize its free energy. Evaluation of the integral for large K yields $\overline{\langle u\rangle\Delta} \approx -(\ln 2/2)K^{-1}$, hence at low temperatures the entropic smoothening of the quenched disorder dominates over the entropic roughening, and the height-difference correlation function *decreases* with increasing temperature as $C(r)/|r| \approx 1/12 - (\ln 2 - 1/2)K^{-1}$. This regime terminates in a minimum at a temperature $K^{-1} \approx 0.1$. With further increase of the temperature the disorder becomes decreasingly significant and the correlations approach those of the SOS model (Fig. 2).

3 Relaxation to equilibrium

3.1 Surface diffusion dynamics

Surface diffusion is introduced into the DSOS model by specifying the rate at which the topmost particle in a column can move to the neighboring sites. Jumps are attempted to the right with probability p and to the left

with probability $1-p$. In equilibrium $p = 1/2$, while in the presence of an external field E the bias is determined through a local detailed balance relation [24] of the form

$$p/(1-p) = \mathrm{e}^{E}. \tag{12}$$

An attempted jump $i \to j$ is accepted with a probability Γ_{ij}, which has to be chosen such that detailed balance with respect to $\mathcal{H}_{\mathrm{DSOS}}$ is satisfied when $E = 0$. Two choices will be considered in this paper.

For Arrhenius dynamics the jump rate is

$$\Gamma_{ij} = \mathrm{e}^{-2Kn_i}, \tag{13}$$

where n_i is the lateral coordination number of the atom at its initial site i. In the SOS model $n_i = 0$, 1 or 2, while in the disordered case n_i is a real number between 0 and 2 which measures the length of the vertical edges that the square representing the atom shares with its neighbors (Fig. 1); equivalently, $2K(n_i-1)$ is the evaporation energy required to remove a particle from column i [16].

An artificial feature of Arrhenius dynamics is that the jump rate is independent of the environment of the target site of the move. In this sense Metropolis dynamics defined by

$$\Gamma_{ij} = \min[1, \mathrm{e}^{-\Delta\mathcal{H}^{ij}_{\mathrm{DSOS}}}] \tag{14}$$

is more realistic, because the difference in the total surface energy $\Delta\mathcal{H}^{ij}_{\mathrm{DSOS}}$ before and after the jump depends on both sites involved.

3.2 Adatom mobility and profile relaxation

On scales very much larger than the lattice constant the relaxation of the DSOS surface towards equilibrium can be described through the continuum equation (2). The thermodynamic driving force is provided by the surface stiffness, which has already been identified in the previous section. The adatom mobility σ can be formally defined through the excess mass current J_E caused by an external bias field E in the zero field limit, as [16,25]

$$\sigma = \lim_{E\to 0} E^{-1} J_E. \tag{15}$$

On the level of linear response a Green-Kubo formula for σ is obtained [25], which involves the thermally averaged jump rate and a correction term given by a space-time integral over the stationary current-current correlation function. For Arrhenius dynamics the correction term vanishes identically [16]. Moreover the thermal average of the jump rate can be carried out in the same way as for the ordered system [16,23], which leads to the result

$$\sigma_{\mathrm{Arr}} = \frac{1}{2}\langle \mathrm{e}^{-2Kn_i}\rangle = \frac{1}{2}\mathrm{e}^{-2K} \tag{16}$$

independent of the local phase shift Δ_i, and independent of the surface slope. Since the mobility is the same for all configurations of phases, a disorder average is not necessary.

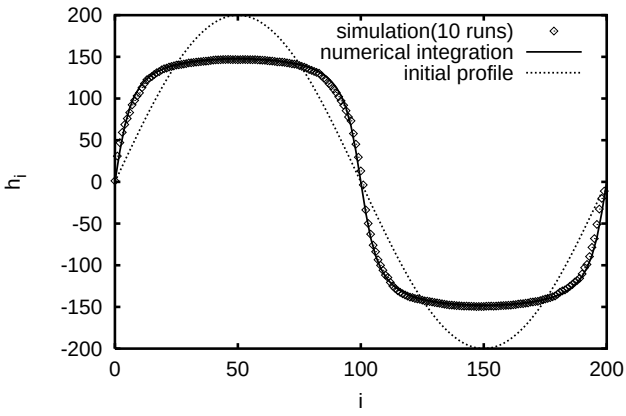

Fig. 3. Flattening of an initially sinusoidal profile after 10^9 MCS at $K = 4$. The figure compares direct simulation using Arrhenius rates with the numerical integration of the continuum equation.

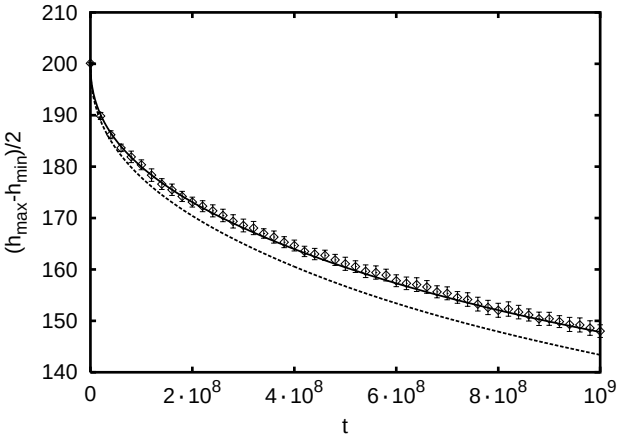

Fig. 4. Time evolution of the peak-to-valley amplitude of the profile shown in Figure 3. The simulation (diamonds) agrees with the numerical integration using the stiffness definition (6) (full line) and rules out the stiffness obtained as the disorder average of the inverse slope variance (dashed line). The error bars indicate statistical errors from 10 independent runs.

With the exact expressions (16) for the mobility and (7, 8) for the stiffness, the continuum equation (2) is fully determined for Arrhenius dynamics, and can be used to predict the large scale evolution of surface profiles in the DSOS model. In Figure 3 this is illustrated for the relaxation of an initially sinusoidal profile. An impressive agreement is reached, without any adjustable parameters. A more sensitive check is provided by the time evolution of the peak-to-valley amplitude $(h_{\max} - h_{\min})/2$ (Fig. 4). This figure clearly demonstrates the correctness of the disorder average leading to the expression (8) for the surface stiffness, and rules out the alternative averaging procedure mentioned in Section 2.1.

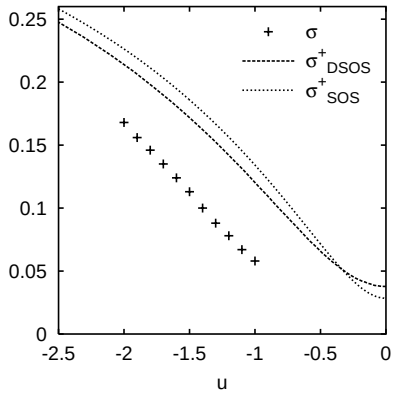

Fig. 5. Crosses show the inclination dependence of the Metropolis mobility, as determined from the excess mass current. The lines show the upper bound σ^+ with and without disorder. The dimensionless inverse temperature is $K = 2$.

To determine the adatom mobility for the choice of Metropolis dynamics one has to rely on simulation, because a direct evaluation is ruled out by the non-vanishing Green-Kubo integral. Without further investigations one can only conclude that the average of the jump rate with respect to the thermal equilibrium state of the DSOS model,

$$\sigma_i^+ = \frac{1}{2}\langle \Gamma_{ii+1} \rangle, \tag{17}$$

represents an upper bound on the true mobility, because the Green-Kubo integral has a definite sign. Correspondingly $\overline{\sigma^+}$ is an upper bound on the disorder averaged mobility. The most direct method for the numerical determination of σ is provided by the basic definition (15) of the mobility through the excess mass current. Counting the difference of particle hops to the left and right and plotting it *versus* the field E yields for a sufficiently small field the expected linear behavior. Figure 5 shows the results for the Metropolis mobility obtained using this method for several inclinations u, compared with the upper bound σ^+ in the ordered and disordered case. Several remarks are in order: (i) Admittedly the upper bound is not exceeded, but it is a poor approximation to the true mobility (for higher temperatures it is more useful). (ii) The differences between the system with and without disorder are small (at least with respect to the upper bound). (iii) There is no fixed relation between mobilities of the ordered and the disordered system. The DSOS mobility is larger for $u \approx 0$ but smaller elsewhere.

3.3 Roughening dynamics

On mesoscopic scales the relaxation into equilibrium starting from a nonequilibrium initial condition, such as $h_i \equiv 0$, is associated with the dynamic buildup of the roughness discussed in Section 2.2. This is most conveniently modeled through a Langevin equation obtained by linearizing the continuum equation (2) around the macroscopically flat profile and adding appropriate noise terms [16]. In addition to a fluctuating current $j_{\rm F}(x,t)$ describing the hopping of adatoms, for the DSOS model one expects also a spatially random, time-independent term describing the quenched random phases [12]. Without loss of generality this can be introduced through a Gaussian quenched random chemical potential $\mu_{\rm R}(x)$. The full Langevin equation then reads

$$\frac{\partial h}{\partial t} = -\overline{\sigma}\frac{\partial^2}{\partial x^2}\left(\overline{\hat{\gamma}}\frac{\partial^2 h}{\partial x^2} - \mu_{\rm R}(x)\right) - \frac{\partial}{\partial x} j_{\rm F}(x,t), \tag{18}$$

where $\overline{\sigma}$ and $\overline{\hat{\gamma}}$ are constants evaluated at the macroscopically imposed slope, and $j_{\rm F}(x,t)$ is white noise in space and time. Thermal and disorder averages now correspond to averaging with respect to $j_{\rm F}$ and $\mu_{\rm R}$, respectively.

The statistics of $\mu_{\rm R}(x)$ is fixed by noting that the thermally averaged equilibrium height profile of the DSOS model $\langle h(x,t)\rangle$ has the same qualitative roughness properties as an equilibrium interface, since the thermally average slopes $\langle u_i \rangle$ are uniquely determined by the phase shifts Δ_i, which are independent at different sites. Thus on large scales $\partial\langle h(x,t)\rangle/\partial x$ has the statistics of spatial white noise. Within the Langevin description of equation (18) the thermally averaged profile is obtained by setting the total chemical potential $\mu + \mu_{\rm R} = -\hat{\gamma}\partial^2 h/\partial x^2 + \mu_{\rm R}$ to zero. It follows that $\mu_{\rm R}$ has zero mean, and its covariance function is of the form

$$\overline{\mu_{\rm R}(x)\mu_{\rm R}(x')} = -D_\mu \frac{\partial^2}{\partial x^2}\delta(x-x'), \tag{19}$$

where the amplitude D_μ can in principle be computed from the formulae given in Section 2.

The solution of (18) is straightforward by Fourier transformation. One finds that the two noise sources $j_{\rm F}$ and $\mu_{\rm R}$ give comparable contributions to the surface width, which grows as $W(t) \sim t^{1/8}$ like in the ordered system [16]. The quenched disorder does not qualitatively change the roughening behavior. This is confirmed by numerical measurements of the surface width, which for the DSOS model is defined by

$$W^2 = \frac{1}{L}\sum_{i=1}^{L}(h_i + \phi_i - \overline{h})^2,$$
$$\overline{h} \equiv \frac{1}{L}\sum_{i=1}^{L} h_i + \phi_i. \tag{20}$$

The data displayed in Figure 6 show that the prefactor of the $t^{1/4}$-law is generally increased by the disorder. This is plausible in view of the expression for the surface width obtained in the absence of disorder [16],

$$W^2(t) \simeq \frac{(2\sigma\hat{\gamma})^{1/4}\Gamma(3/4)}{\pi\hat{\gamma}} t^{1/4}. \tag{21}$$

It shows that the prefactor is primarily determined by the stiffness $\hat{\gamma}$, which is reduced by the disorder (see Sect. 2).

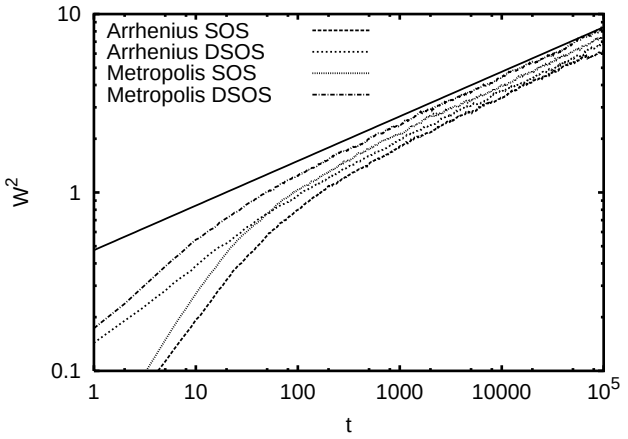

Fig. 6. Roughening dynamics of an initially flat surface. The figure shows simulation data for the surface width obtained using Arrhenius and Metropolis dynamics in the presence and absence of disorder. The full line indicates the predicted $t^{1/4}$-power law.

4 Driven surface diffusion

4.1 Random mobility and disorder-induced roughening

While in the preceding section the infinitesimal bias field E was introduced only as a theoretical device in the definition of the adatom mobility, here we want to examine the nonequilibrium steady state which is generated by imposing a finite bias $E > 0$ in (12). Provided the bias is not too strong, the induced additional current can be written as $J_E = \sigma E$. Through the dependence of the adatom mobility on the surface morphology this may couple to the surface dynamics. As discussed in Section 3, there is no such dependence in the case of Arrhenius dynamics; therefore in the following we consider only Metropolis dynamics.

In the absence of disorder, the main effect of the field is obtained by linearizing the corresponding term $-\partial J_E/\partial x$ appearing on the right hand side of the continuum equation (2) around a profile of constant slope u. This yields a second order derivative term $-E\sigma'(u)\partial^2 h/\partial x^2$, where $\sigma'(u) = \mathrm{d}\sigma/\mathrm{d}u$. If $E\sigma'(u) > 0$, fluctuations like valleys or hills are not flattened out but amplified, ending up in a faceted surface, while for $E\sigma'(u) < 0$ the surface is stabilized by the field [19,20]. While the faceting transition persists in the DSOS model [23], the more interesting disorder effects appear in the stabilizing case, which we now investigate. For both SOS and DSOS models the stable regime appears for sufficiently negative slopes [19,20]; in the following we typically choose a mean slope $u = -1$, which is fixed through helical boundary conditions.

In the presence of disorder we expect the random phases to induce a spatially fluctuating contribution to the mobility. Microscopically, the mobility at site i depends on three neighboring phase shifts $\Delta_{i-1,i,i+1}$. Numerical investigations of the statistics of the upper bound (17) indicate that the fluctuations in the mobility are uncorrelated beyond a few lattice constants, and moreover they depend only weakly on inclination in the parameter range of interest [23]. We therefore separate the spatial dependence from the inclination dependence, and make the following ansatz for the adatom mobility in the continuum description of the driven DSOS model,

$$\sigma(\nabla h, x) = \bar{\sigma}(\nabla h) + \sigma_{\mathrm{R}}(x). \tag{22}$$

Here $\bar{\sigma}$ denotes the average, space-independent contribution which appears in the SOS model as well, and $\sigma_{\mathrm{R}}(x)$ is a quenched Gaussian random variable with zero mean and covariance

$$\overline{\sigma_{\mathrm{R}}(x)\sigma_{\mathrm{R}}(x')} = \Sigma\delta(x - x'). \tag{23}$$

We have attempted to numerically estimate the amplitude Σ from the variance of the upper bound σ_i^+, which unfortunately gives reasonable results for high temperatures only; in the following Σ will therefore be treated as a free parameter of the theory.

Collecting all relevant terms, the Langevin equation describing the surface fluctuations in the field driven SOS and DSOS models reads

$$\frac{\partial h}{\partial t} = -\bar{\sigma}\bar{\hat{\gamma}}\frac{\partial^4 h}{\partial x^4} - E\bar{\sigma}'\frac{\partial^2 h}{\partial x^2} - E\frac{\partial \sigma_{\mathrm{R}}}{\partial x} - \frac{\partial j_{\mathrm{F}}}{\partial x}. \tag{24}$$

In the presence of the field-induced second order derivative term, the quenched random chemical potential μ_{R} appearing in (18) is irrelevant compared to the other noise sources. Also the first, fourth order derivative term on the right hand side of (24) is irrelevant for the long wavelength behavior, however it is needed as a short wavelength regularization for the ordered case (see below).

If we assume equilibrium statistics for the fluctuating current $j_{\mathrm{F}}(x,t)$, choosing its covariance according to the fluctuation-dissipation theorem as [16]

$$\langle j_{\mathrm{F}}(x,t) j_{\mathrm{F}}(x',t')\rangle = 2\bar{\sigma}\delta(x - x')\delta(t - t'), \tag{25}$$

the solution of (24) yields the expression

$$W^2(t) \simeq (2 - \sqrt{2})\Sigma\sqrt{\frac{E}{\pi|\bar{\sigma}'|^3}}t^{1/2} + \frac{1}{2\bar{\hat{\gamma}}}\sqrt{\frac{\bar{\sigma}\bar{\hat{\gamma}}}{|\bar{\sigma}'|E}} \tag{26}$$

for the asymptotic behavior of the surface width.

For the ordered SOS model ($\Sigma = 0$, $\bar{\sigma} = \sigma$, $\bar{\hat{\gamma}} = \hat{\gamma}$) the width saturates at a value proportional to $E^{-1/2}$. The field suppresses the thermal surface roughness; the dependence of the saturation width on the surface stiffness $\hat{\gamma}$ reflects the role of the fourth order term in (24) as a short distance regularization. The quenched disorder destroys the saturation of W, leading to a roughness evolution $W \sim t^{1/4}$ which is faster than the $t^{1/8}$-law of thermal roughening (Sect. 3.3). Due to the non-homogeneous mobility the field induces a corresponding spatially fluctuating current, which drives the surface into a steady state with a space-independent current. This is achieved by building up a certain surface profile which is determined by the disorder (see Sect. 4.2). Note that the coefficient of the leading $t^{1/2}$-behavior in (26) is independent

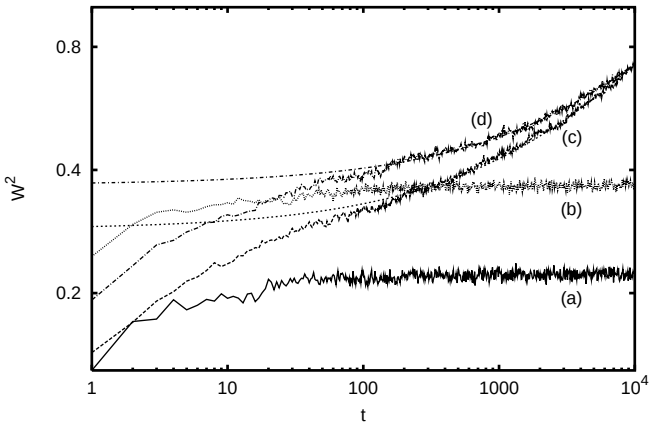

Fig. 7. Saturation of the surface width for the field-driven ordered surface of length $L = 10\,000$ at $K = 3$ and $u = -1$ for field strength (a) $E = 2$ and (b) $E = 1$. In the disordered system with the same parameters (c) $E = 2$ and (d) $E = 1$ the surface roughens at late times. The fits are of the form $a + bt^{1/2}$.

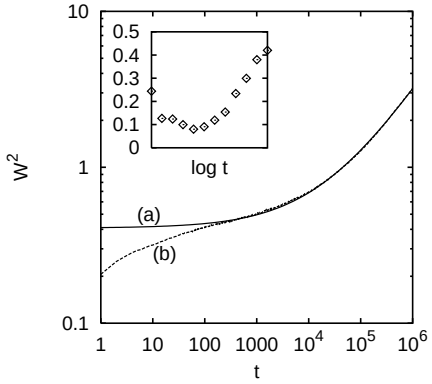

Fig. 8. Disorder-induced roughening for a large system ($L = 10^5$) at field strength $E = 0.5$, $K = 4$ and slope $u = -1$. The numerical data (curve (b)) are compared to a fit of the form $a + bt^{1/2}$ (curve (a)). The inset shows the effective exponent $\alpha(t)$ defined by $W^2(t) = a(t_0)t^{\alpha(t_0)}$ in the neighborhood of a time t_0. For late times one expects $\alpha \to 1/2$.

of both $\bar{\tilde{\gamma}}$ and $\bar{\sigma}$, which shows that the asymptotics of the width is determined only by the second and third terms on the right hand side of (24).

Figure 7 shows simulation results for the surface width[1] in the driven SOS and DSOS models. The agreement with the predicted $t^{1/2}$-law for the disordered case is very good. The prefactor is expected to be proportional to $E^{1/2}$, thus the ratio of the prefactors in the two cases approximates the value $\sqrt{2}$. Further quantitative comparison with the theory would require a better knowledge of Σ [23]. The evolution of a much larger system is shown in Figure 8. Again the excellent agreement supports our ansatz (22) for the random mobility.

[1] Note that in the case of inclined surfaces the mean tilt has to be subtracted prior to the evaluation of the surface width (20).

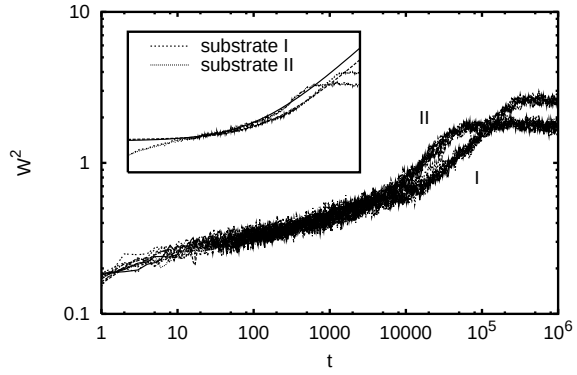

Fig. 9. Disorder-induced roughening in small systems ($L = 500$, $K = 4$, $E = 1$, $u = -1$) for two different disorder configurations. 10 independent runs were carried out for each configuration. The inset shows the averages over the two sets of runs together with fits of the form $a + bt^{1/2}$.

4.2 Sample-to-sample fluctuations and the steady state surface profile

For small systems we observed large sample-to-sample fluctuations of the surface width. In Figure 9 the roughness evolution is shown for two different disorder configurations in a system of size $L = 500$. The saturation of the surface width at long times is a finite-size effect; the solution of the Langevin equation (24) shows that the width saturates at a value $W_\infty(L) = \sqrt{\Sigma L/12|\bar{\sigma}'|^2}$. The more remarkable feature of the data shown in Figure 9 is that the fluctuations between different runs in the same disorder environment are much smaller than the sample-to-sample fluctuations between the two different environments. Indeed, when considering the height difference between two different runs in the same environment, the random mobility term in (24) cancels and the equation reduces to that for the ordered, driven SOS model, which has bounded surface fluctuations.

To understand in more detail which features of the phase disorder configuration determine the roughness evolution, it is useful to compare the steady state height profiles which are established for times beyond the saturation time (Fig. 10). A Fourier analysis shows that for the disorder configuration I (upper panel) the dominant Fourier mode is $q = 2\pi/L$, while in configuration II (lower panel) the mode $q = 4\pi/L$ dominates. This means that in configuration II the typical distance over which particles have to be moved to build up the steady state profile is smaller, and therefore the roughening dynamics is faster. On the other hand in configuration I the long wavelength modes have a larger amplitude, and correspondingly the saturation value W_∞^2 is larger in that case. Thus the main qualitative features of the different roughness evolutions seen in Figure 9 can be explained by inspection of the steady state profile.

Since the steady state height profile is uniquely determined by the random phases, it would be highly desirable

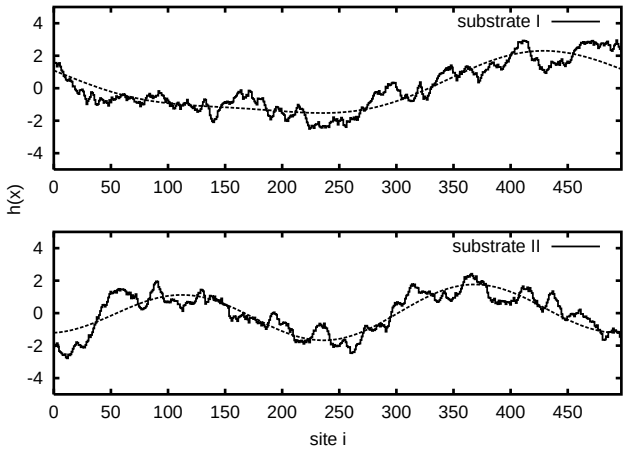

Fig. 10. Stationary surface profiles for the two disorder configurations of Figure 9. The smooth curves show the combination of the lowest Fourier modes with $q = 2\pi/L$ and $q = 4\pi/L$.

to be able to compute it directly without having to simulate the time-dependent process. Inspired by a related approach used in a recent study of disordered exclusion models [26], we have developed an approximate scheme for the calculation of the steady state profiled based on the following rate equations for the thermally averaged local slope in the DSOS model:

$$\frac{\mathrm{d}}{\mathrm{d}t}\langle u_i(t)\rangle = \langle p(2\Gamma_{i-1,i} - \Gamma_{i,i+1} - \Gamma_{i-2,i-1})\rangle + \langle (1-p)(\Gamma_{i+1,i} + \Gamma_{i-1,i-2} - 2\Gamma_{i,i-1})\rangle. \quad (27)$$

If the averages $\langle\cdot\rangle$ were taken with respect to the (unknown) true nonequilibrium steady state of the system, equation (27) would be exact. Our approximation consists of using instead the thermally averaged equilibrium jump rates

$$\langle\Gamma_{i,i+1}\rangle = \frac{1}{Z}\sum_{\substack{u_i,u_{i+1},\\ u_{i+2}=-\infty}}^{\infty} \exp\{-\mathcal{H}\}\min(1,\exp\{-\Delta\mathcal{H}\}), \quad (28)$$

where Z is the partial partition function for the three neighboring slope variables and $\Delta\mathcal{H}$ is the energy change associated with the particle hopping. Both $\mathcal{H}$ and $\Delta\mathcal{H}$ depend on the slope chemical potentials m_i, m_{i+1}, m_{i+2} and the disorder parameters $\Delta_i, \Delta_{i+1}, \Delta_{i+2}$ of three neighboring sites. The functional relation between $\langle u_i\rangle$ and m_i at given Δ_i can be inverted numerically, thus (28) can be written in the form

$$\langle\Gamma_{i,i+1}\rangle = F(\Delta_j, \langle u_j\rangle | j = i-2, \ldots, i+2). \quad (29)$$

In this approximation equation (27) reduces to a system of L coupled, non-linear equations for the expectation values of u_i, which can be solved by iteration. The initial profile is chosen as the constant slope configuration.

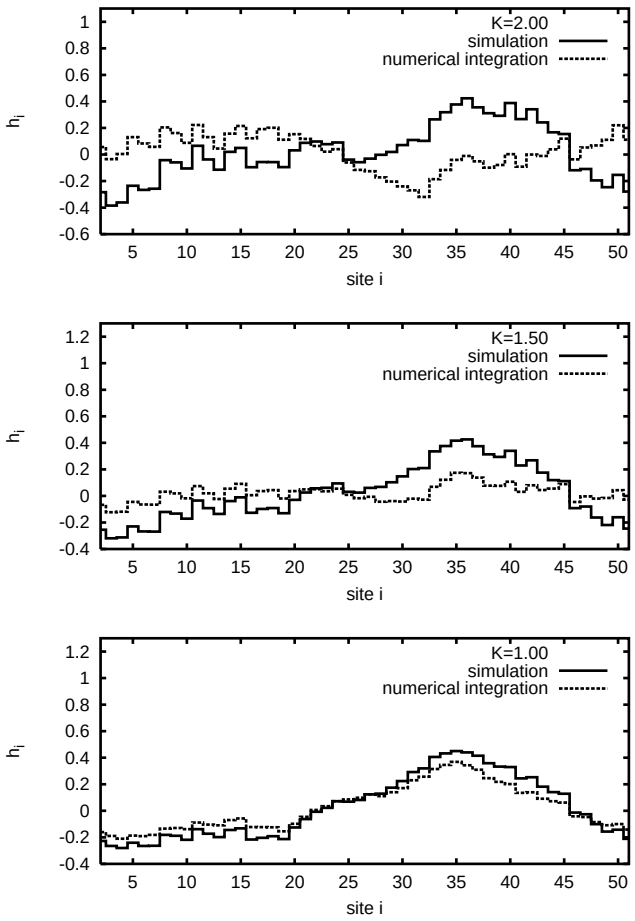

Fig. 11. Comparison of stationary profiles obtained by direct simulations and by numerical solution of the approximate rate equations for different temperatures. In all cases $L = 50$, $E = 1$ and $u = -1$.

In Figure 11 the approximate profiles are compared to those obtained from direct simulation. The agreement is quite satisfactory for $K = 1.00$, becoming worse with decreasing temperature. For $K = 1.50$ and $K = 2.00$ there are still local similarities, but also stretches along which the slope of the approximate profile seems to be the *negative* of the true one. We have checked that the explanation for this curious phenomenon does not lie in the existence of multiple, symmetry-related steady state solutions of equations (27): Even if the numerical solution of the rate equations is started with the final profile of the direct simulation, one ends up in exactly the same final state.

5 Conclusions

In this paper we have explored the effects of a certain type of structural disorder on the behavior of one-dimensional SOS surfaces. While the static roughness of the model could be treated exactly, the dynamic fluctuations were analyzed in the framework of phenomenological Langevin

equations. In these equations (Eqs. (18, 24)) the disorder introduces noise terms – chemical potentials and currents – which are random in space but independent of time. In the absence of a driving field the quenched disorder was found to be marginal, in the sense that it leads to the same kind of roughening dynamics as the time-dependent fluctuations in the ordered system, while the combination of random mobilities and a driving field was shown to induce a novel roughening mechanism.

Similar Langevin equations with quenched random forces have been extensively studied in the context of charge density waves, driven flux line lattices and related condensed matter systems [11,12,21,22]. Our problem is simpler in that easily solvable *linear* equations suffice for an accurate description of the behavior, because no relevant nonlinearities exist.

An interesting extension of the present work would be to consider the combination of deposition and surface diffusion in the DSOS model. Similar to the behavior in the ordered SOS model [27], the deposition flux may induce surface currents which however in the disordered system would be random in space. Possibly such effects could contribute to the morphological instability which has been observed in the growth of amorphous thin films [7].

Thanks are due to Andy Zangwill for asking a question which motivated this work. The support of DFG within SFB237 *Unordnung und grosse Fluktuationen* is gratefully acknowledged.

References

1. W.W. Mullins, J. Appl. Phys. **30**, 77 (1959).
2. R.M. Bradley, J.M.E. Harper, J. Vac. Sci. Technol. A **6**, 2390 (1988).
3. M. Schimschak, J. Krug, J. Appl. Phys. **87**, 695 (2000).
4. T. Ala-Nissila, S.C. Ying, Prog. Surf. Sci. **39**, 227 (1992).
5. I. Avramov, J. Phys. Cond. Matter **11**, L267 (1999).
6. H.-N. Yang, Y.-P. Zhao, G.-C. Wang, T.-M. Lu, Phys. Rev. Lett. **76**, 3774 (1996).
7. B. Reinker, M. Moske, K. Samwer, Phys. Rev. B **56**, 9887 (1997).
8. J.P. Bouchaud, A. Georges, Phys. Rep. **195**, 127 (1990).
9. J. Krug, in *Nonequilibrium statistical mechanics in one dimension*, edited by V. Privman (Cambridge University Press, 1997), p. 305.
10. J. Krug, in *Surface Disordering: Growth, Roughening and Phase Transitions*, edited by R. Jullien, J. Kertész, P. Meakin, D.E. Wolf (Nova Science, New York 1992), p. 177.
11. D. Cule, Y. Shapir, Phys. Rev. Lett. **74**, 4133 (1994).
12. J. Krug, Phys. Rev. Lett. **75**, 1795 (1995).
13. J. Toner, D. Di Vincenzo, Phys. Rev. B **41**, 632 (1990).
14. H. Rieger, U. Blasum, Phys. Rev. B **55**, R7394 (1997).
15. For a review see Y. Shapir, in *Dynamics of fluctuating interfaces and related phenomena*, edited by D. Kim, H. Park, B. Kahng (World Scientific, Singapore 1997), p. 245.
16. J. Krug, H.T. Dobbs, S. Majaniemi, Z. Phys. B **97**, 281 (1995).
17. P.S. Ho, T. Kwok, Rep. Prog. Phys. **52**, 301 (1989).
18. H. Yasunaga, A. Natori, Surf. Sci. Rep. **15**, 205 (1992).
19. J. Krug, H.T. Dobbs, Phys. Rev. Lett. **73**, 1947 (1994).
20. H. Dobbs, J. Krug, J. Phys. I France **6**, 413 (1996).
21. L. Balents, M.P.A. Fisher, Phys. Rev. Lett. **75**, 4270 (1995).
22. S. Scheidl, V.M. Vinokur, Phys. Rev. E **57**, 2574 (1998); L. Balents, M.C. Marchetti, L. Radzihovsky, Phys. Rev. B **57**, 7705 (1998).
23. U. Börner, Diploma thesis, University of Essen, 1999.
24. S. Katz, J. Lebowitz, H. Spohn, J. Stat. Phys. **34**, 497 (1984).
25. H. Spohn, J. Stat. Phys. **71**, 1081 (1993).
26. G. Tripathy, M. Barma, Phys. Rev. E **58**, 1911 (1998).
27. J. Krug, M. Plischke, M. Siegert, Phys. Rev. Lett. **70**, 3271 (1993).